Re-Entry Trajectory Tracking Via an Inverse Dynamics Method

Dae-Woo Lee*, **Kyeum-Rae Cho**
Department of Aerospace Engineering Pusan National University, Research Institute of Mechanical Technology, Jangjun-Dong, Kumjung-Ku, Pusan, #609-735, Korea
Hui Yan
Department of Mathematics, Texas A&M, #77843, USA

Atmospheric Re-Entry guidance is divided as longitudinal and lateral. This paper proposes a longitudinal reference trajectory and control law using the inverse dynamics method with pseudospectral Legendre method. Application of this method into Re-Entry problem forces a power of calculation time-reduction due to unnecessary of integration or any iteration as well as sufficient accuracy convergence. The used guidance scheme is time-to-go.

Key Words: Atmospheric Re-Entry (RE), Reference Trajectory, Tracking, Pseudospectral Legendre Method, Inverse Dynamic Method, Linear Algebraic Equations

1. Introduction

Reviewing the space-technological history of human, there was a great revolution for a short period of time. Russia had launched the first satellite in Oct. 1957. And in July 1969, Apollo 11 achieved the dream of human landing on the moon. According to the history of science, the development and employment of various satellite missions such as science, communication, observation etc. become more important. The previous profile of the satellite orbit entry consists of the loading of the satellite in the launch vehicle, launch, de-orbit, separation from the launch vehicle, and orbit entry for a mission performance. The launch vehicle separates sequentially the multi-step rockets and the fuel tank from the main module until an ejection of satellite. The last remained module becomes the space waste. Thus, economic problem is considerable point due to large number of launches. To sustain the variety and the precision of space-technology with the acceleration of the times, space development becomes an activity that needs system arrangement with the economy. For this reason, a new generation reusable payload vehicles have been developed in several countries. Herein, the guidance problem for a RE vehicle is difficult because it will have limited control (i.e., L/D). The density and winds along its RE trajectory are unpredictable, and there will be a high accuracy requirement for RE and recovery.

The main idea of the RE guidance is to set up a reference drag acceleration profile within the permissible entry corridor, adjust and track this profile, many researchers made a lot of improvements on the RE scheme. For example, calculus of variation (COV) algorithms have been considered by Baker, Causey and Ingram, 1971. In 1983, Harpold and Graves, Jr. analyzed the reference trajectory by dividing each segment according into the predominant constraints. And Alberto Cavallo proposed an LQR control scheme for RE in 1996. Although several work

* Corresponding Author,
E-mail: baenggi@pusan.ac.kr
TEL: +82 51-510-2329; **FAX**: +82-51-513 3760
Department of Aerospace Engineering Pusan National University, Research Institute of Mechanical Technology, Jangjun-Dong, Kumjung-Ku, Pusan, #609-735, Korea. (Manuscript **Received** August 12, 2003; **Revised** May 31, 2004)

was dedicated to determine the RE guidance using optimal control methods, very few papers studied the on-line RE guidance.

This paper proposes the RE guidance system (Lee and Cho, 2002) for the RLV (Reusable Launch Vehicle) via efficient algorithms with Spectral Legendre methods so that the idea can be used for on-line RE guidance. Legendre polynomial is one of global orthogonal polynomials like Chebyshev (Lee, 2003). These polynomials are used extensively in spectral methods for solving fluid dynamic problem, but their use in solving optimal control problems has created a new way of transforming them to NLP problem. Its particular merit is its close relationship to Gauss-type integration rules. This relationship can be derived simple rule for transforming the original optimal control problem to a system of algebraic equations. The main idea of this algorithm is to reduce an optimal control problem to algebraic equations. Therefore, because the guidance law obtained from this process does not need any integrations or iterations, this scheme can be rapidly performed in the real time manner.

2. Generation of a Reference Trajectory

2.1 Dynamics of re-entry

Because the RE flight (Regan and Anandakrishnan, 1993) for the space vehicle follows after the ascent flight, the design of ascent and RE trajectories are carried out simultaneously. The dimensionless equations of motion (Roenneke, 1993; Cavallo, 1996; Lu. 1997) of the RE vehicle can be described under the following assumptions, and considered as a nonlinear time-varying system.

1. The earth is assumed to be a non-rotating sphere.

2. The non-thrusting RE space vehicle is assumed as a point mass from the vertical plane of the earth.

$$\dot{r}=v\sin\gamma \tag{1}$$

$$\dot{v}=-D-\frac{\mu}{r^2}\sin\gamma \tag{2}$$

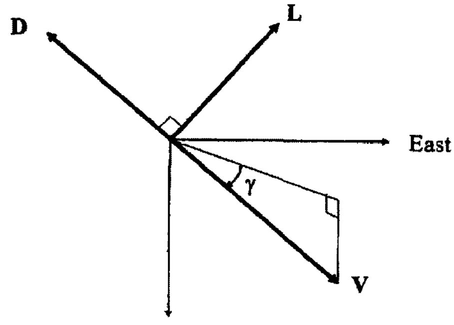

Fig. 1 Vectors for the RE vehicle

$$\dot{\gamma}=\frac{D}{v}u+\left(v^2-\frac{\mu}{r}\right)\frac{\cos\gamma}{rv} \tag{3}$$

$$D=\frac{\rho S v^2 C_D}{2m},\ L=\frac{\rho S v^2 C_L}{2m} \tag{4}$$

$$u=\frac{C_L}{C_D}\cos\sigma \tag{5}$$

where r is the radial distance from the earth center to the RE vehicle, normalized by the earth radius r_E, the Earth-relative velocity v is normalized by $\sqrt{g_0 r_E}$ (g_0 is gravitational acceleration at sea level). γ is the flight path angle, μ is defined as the gravity constant, μ/r^2 can be described as the gravity acceleration g. Aerodynamic acceleration D and L are normalized by g_0. The control variable u can be defined as the function of the bank angle σ and the vertical component of the lift-to-drag ratio. The drag coefficient is C_D, the dynamic pressure q, the reference area S, the mass m, the lift coefficient C_L and the atmospheric density ρ.

We should notice the angle of attack α is selected in preflight. Fig. 1 shows the vectors for the RE vehicle.

2.2 Constraints

The reference drag acceleration is defined within the RE corridor which means a permissible flight corridor. This RE corridor for the RLV must satisfy the following trajectory constraints (Lu, 1997).

1) Heating rate constraint

The heating rate (Incropera and DeWitt, 1985) is decided by the performance of the protective heat tiles because it is proportional to the temperature of the outside surface. From the definitions

$$D \le \frac{C_D S}{2mv^4} \dot{Q}_{\max}^2 \tag{6}$$

where $\dot{Q}_{\max}=3.305\times 10^9$.

2) Normal load factor constraint

The load factor normal to the airframe is decided by the acceleration which human or the structure of the airframe or the instrument can bear.

$$D \le \frac{g_0 n_{\max}}{C_L/C_D \cos\alpha + \sin\alpha} \tag{7}$$

where the maximum load factor $n_{\max}=2$, α is angle of attack.

3) Equilibrium glide constraint

The equilibrium glide constraint is the limit in which the re-entry vehicle can fly without nose-down at zero-bank angle. From the definition

$$D \ge \frac{C_D}{C_L}\left(g - \frac{v^2}{r}\right) \tag{8}$$

4) Dynamic pressure constraint

It is applied at low-speeds of re-entry. If the dynamic pressure constraint exceeds the limit, the control surface returns to neutral condition in spite of operating at the control surface. The condition for maximum dynamic pressure provides

$$D \le \frac{S C_D q_{\max}}{m} \tag{9}$$

where the maximum allowable dynamic pressure $q_{\max}=16{,}280\,(\mathrm{N/m^2})$.

5) Range constraint

The objective of the range error constraint is such that the difference between the actual range s, and the pre-designed range s_{ref} is zero. From the definition of time derivative of range

$$\dot{s} = v\cos\gamma \tag{10}$$

Integrating this with respect to t and replacing the integration variable with γ using Eq. (2) result in

$$s = \int_{t_0}^{t_f} v\cos\gamma dt = \int_{v_0}^{v_f} \frac{v\cos\gamma}{-D-g\sin\gamma} dv \tag{11}$$

Since γ is small we can write the range as

$$s = \int_{v_0}^{v_f} -\frac{v}{D} dv \tag{12}$$

2.3 Performance index

The control of an angle of attack has an efficient in high frequency domain. However, assuming the total heating can be reduced by selecting a proper angle of attack, the only inclination of drag acceleration with respect to velocity can be considered as the performance index:

$$J = \min \int_{v_0}^{v_f} D'(v)^2 dv \tag{13}$$

2.4 Permissible flight corridor for re-entry

The re-entry trajectory is limited by the constraints that determine the magnitude of the drag acceleration. The re-entry corridor is also defined by these constraints. Therefore, drag accelerations at each node satisfy Eq. (14) which is defined as the minimum and the maximum drag acceleration in each node. It is also converted by a transformation of Eq. (15). D_0 and D_f are fixed values which are obtained from the definition of drag acceleration. Because they satisfy a prescribed flare maneuver.

$$\begin{gathered} D_{lb}(v_l) \le D(v_l) \le D_{ub}(v_l) \\ D(v_0) = D_0,\ D(v_f) = D_f \end{gathered} \tag{14}$$

$$\begin{gathered} D_l = D_{lb}(v_l) + 0.5\times[D_{ub}(v_l) - D_{lb}(v_l)], \\ l = 0, 1, 2, \cdots, f \end{gathered} \tag{15}$$

3. Longitudinal Control via Inverse Dynamics Method

In this section, we present inverse dynamics method (Kim and Ryu, 2002). The guidance system also consists of longitudinal guidance and lateral guidance. The former has two parts, one generates the reference drag acceleration which is based on the states and the other is the trajectory control which is acquired by the attitude angle needed to track the reference trajectory. From the definition of drag acceleration Eq. (4), the first derivative of D with respect to v is

$$D'=\frac{2D}{v}+\frac{D}{\rho}\rho'+\frac{D}{C_D}C_D' \tag{16}$$

Replacing ρ' by exponential atmosphere model (Regan, 1993), Eq. (16) is

$$D'=\frac{2D}{v}-r'D\beta+\frac{D}{C_D}C_D' \tag{17}$$

Form Eqs. (1) and (2), since γ is very small for atmospheric re-entry,

$$r'=-\frac{v\gamma}{D+g\gamma}\approx-\frac{v\gamma}{D} \tag{18}$$

Substituting Eq. (18) for r' in Eq. (17),

$$D'=\left(\frac{2}{v}+\frac{C_D'}{C_D}\right)D+v\beta\gamma \tag{19}$$

Second derivatives of D from Eq. (19)

$$\begin{aligned} D''=&\frac{2(D'v-D)}{v^2}+\frac{(D'C_D-C_D'D)C_D'}{C_D^2}\\ &+\frac{DC_D''}{C_D}+v\beta\gamma'+\beta\gamma \end{aligned} \tag{20}$$

Substituting the first derivative of flight path angle with respect to velocity for time derivatives in Eqs. (2) and (3),

$$\gamma'=-\frac{u}{v}+\frac{g}{vD}-\frac{v}{rD} \tag{21}$$

Replacing Eq. (20) by Eq. (21) and representation about γ in Eq. (19),

$$\begin{aligned} D''=&\left(\frac{C_D'}{C_D}+\frac{3}{v}\right)D'+\beta\left(g-\frac{v^2}{r}\right)\frac{1}{D}\\ &-\left(\frac{4}{v^2}+\frac{C_D'^2}{C_D^2}+\frac{C_D'}{vC_D}-\frac{C_D''}{C_D}\right)D-\beta u \end{aligned} \tag{22}$$

The control variable can be obtained from Eq. (22)

$$\begin{aligned} u=&-\frac{D''}{\beta}+\frac{1}{\beta}\left(\frac{3}{v}+\frac{C_D'}{C_D}\right)D'\\ &-\frac{1}{\beta}\left(\frac{4}{v^2}+\frac{C_D'}{vC_D}+\frac{C_D'^2}{C_D^2}-\frac{C_D''}{C_D}\right)D\\ &+\left(g-\frac{V^2}{r}\right)\frac{1}{D} \end{aligned} \tag{23}$$

4. Discretization Using Orthogonal Polynomials

4.1 Conversion of Dynamics into a TPBVP via Linearization

Equations (1)-(3) can be linearized for the solutions of δu according to Eq. (5). Let $\delta x=(\delta r, \delta v, \delta\gamma)^T$. δx and δu denote the differences between the actual and the nominal values in x and u. The linearized dynamics of Eqs. (1)-(3) can be considered as the general form LTV system as following

$$\delta\dot{x}(\tau)=A(\tau)\delta x(\tau)+B(\tau)\delta u(\tau),\quad 0\leq\tau\leq t_f \tag{24}$$

with the initial conditions

$$x(\tau)=x_0 \tag{25}$$

here, $\delta x(\tau)$, $\delta u(\tau)$, $A(\tau)$, and $B(\tau)$ are $n\times 1$ state vectors, $m\times 1$ control vectors, $n\times n$ matrix and $n\times m$ matrix, respectively. The problem is to determine the optimal control $\delta u(\tau)$ and corresponding state vector $\delta x(\tau)$ satisfying Eqs. (24) and (25) while minimizing the quadratic performance index

$$\begin{aligned} J=&\frac{1}{2}\delta x^T(\tau_f)P_f\delta x(\tau_f)\\ &+\frac{1}{2}\int_{\tau_0}^{\tau_f}[\delta x^T(\tau)Q(\tau)\delta x(\tau)+\delta u^T(\tau)R(\tau)\delta u(\tau)] \end{aligned} \tag{26}$$

where P_f and $Q(\tau)$ are $n\times n$ symmetric positive semi-definite matrices and $R(\tau)$ is a $m\times m$ symmetric positive definite matrix.

The Hamiltonian for this system is

$$\begin{aligned} H=&\frac{1}{2}[\delta x^T(\tau)Q(\tau)\delta x(\tau)+\delta u^T(\tau)R(\tau)\delta u(\tau)]\\ &+\delta\lambda^T(\tau)[A(\tau)\delta x(\tau)+B(\tau)\delta u(\tau)] \end{aligned} \tag{27}$$

where $\delta\lambda(\tau)$ are costate vectors.

According to the calculus of variations, we have costate equations

$$\begin{aligned} \delta\dot{\lambda}=&-\frac{\partial H}{\partial\delta x}\\ =&-[Q(\tau)\delta x(\tau)+A^T(\tau)\delta\lambda(\tau)] \end{aligned} \tag{28}$$

and from the necessary optimality conditions $\dfrac{\partial H}{\partial\delta u}=0$

$$\delta u(\tau) = -R^{-1}(\tau) B^T(\tau) \delta\lambda(\tau) \tag{29}$$

The transversality conditions are

$$\delta\lambda(\tau_f) = P_f \delta x(\tau_f) \tag{30}$$

The following linear TPBVP (Two-Point Boundary Value Problem) (Bryson, 1975) can be obtained by substituting Eq. (29) into Eq. (24).

$$\begin{bmatrix} \dot{\delta x} \\ \dot{\delta\lambda} \end{bmatrix} = \begin{bmatrix} A(\tau) & -B(\tau) R^{-1}(\tau) B^T(\tau) \\ -Q(\tau) & -A^T(\tau) \end{bmatrix} \begin{bmatrix} \delta x \\ \delta\lambda \end{bmatrix} \tag{31}$$

4.2 Pseudospectral Legendre Method (PLM)

The collocation type method (Elnagar and Razzaghi, 1997 ; Han et al., 1989) presented in this paper has an objective of finding polynomial approximations for the state, costate and control functions in terms of their values at some carefully chosen Legendre-Gauss-Lobatto (LGL) points. The LTV systems with quadratic criteria can be reduced to solving a system of algebraic equations using this method. To order to use the LGL nodes which lie in the $[-1, 1]$, the time transformation is introduced for $t \in [t_0, t_N] = [-1, 1]$;

$$\tau = \frac{(\tau_f - \tau_0) t + (\tau_f + \tau_0)}{2} \tag{32}$$

It follows that Eq. (31), Eq. (25) and (26) can be replaced by

$$\begin{aligned} \delta\dot{x}(t) = \frac{t_f - t_0}{2} [&A(t) \delta x(t) \\ &- B(t) R^{-1}(t) B^T(t) \delta\lambda(t)] \end{aligned} \tag{33}$$

$$\begin{aligned} \delta\dot{\lambda}(t) = -\frac{t_f - t_0}{2} [&Q(t) \delta x(t) \\ &+ A^T(t) \delta\lambda(t)] \end{aligned} \tag{34}$$

$$\delta x(-1) = x_0 \tag{35}$$

$$\begin{aligned} J = &\frac{1}{2} \delta x^T(1) P_f \delta x(1) \\ &+ \frac{t_f - t_0}{4} \int_{-1}^{1} [\delta x^T(t) Q(t) \delta x(t) \\ &+ \delta u^T(t) R(t) \delta u(t)] \end{aligned} \tag{36}$$

Let L_N be the Legendre polynomial of degree N on the interval $[-1, 1]$;

$$L_N(t) = \frac{1}{2^N} \sum_{l=1}^{N/2} (-1)^l \binom{N}{l} \binom{2N-2l}{N} x^{N-2l} \tag{37}$$

In the Legendre pseudospectral approximation (Sim and Kim, 1996 ; Canuto et al., 1988) of Eq. (33) through Eq. (36), the LGL points are used, t_l, $l=0, \cdots, N$ which are given by $t_0 = -1$, $t_N = 1$. And for $1 \le l \le N-1$, t_l are the zeros of $\dot{L}_N$, the derivative of the Legendre polynomial L_N. There are no closed form expressions for these nodes, and they have to be computed numerically. For approximating the continuous equations, a polynomial approximation form are

$$\begin{aligned} \delta x^N(t) &= \sum_{l=0}^{N} \delta x(t_l) \phi_l(t) \\ \delta u^N(t) &= \sum_{l=0}^{N} \delta u(t_l) \phi_l(t) \\ \delta\lambda^N(t) &= \sum_{l=1}^{N} \delta\lambda(t_l) \phi_l(t) \end{aligned} \tag{38}$$

where for $l=0, 1, \cdots, N$

$$\phi_l(t) = \frac{1}{N(N+1) L_N(t_l)} \frac{(t^2-1) \dot{L}_N(t)}{t - t_l} \tag{39}$$

are the Lagrange polynomials of order N which interpolate the function at the LGL points. The interpolating polynomials satisfy the Kronecker delta. From this property of ϕ_l it follows that

$$\begin{aligned} \delta x^N(t_l) &= \delta x(t_l) \\ \delta u^N(t_l) &= \delta u(t_l) \\ \delta\lambda^N(t_l) &= \delta\lambda(t_l) \end{aligned} \tag{40}$$

Generally the approximations are expressed as

$$\delta x(t) \approx \delta x^N, \ \delta u(t) \approx \delta u^N, \ \delta\lambda(t) \approx \delta\lambda^N \tag{41}$$

but in this collocation method, as stated in the Eq. (40) the values of the approximate state, control and costate functions are given exactly by the value of the continuous functions at these points. Setting $X = (a_0^T, a_1^T, \cdots, a_N^T)$, $U = (b_0^T, b_1^T, \cdots, b_N^T)$, $\Lambda = (c_0^T, c_1^T, \cdots, c_N^T)$, the new notation are

$$a_l := \delta x(t_l), \ b_l := \delta u(t_l), \ c_l := \delta\lambda(t_l) \tag{42}$$

to rewrite Eqs. (40) in the form :

$$\begin{aligned} \delta x^N(t) &= \sum_{l=0}^{N} a_l \phi_l(t) \\ \delta u^N(t) &= \sum_{l=0}^{N} b_l \phi_l(t) \\ \delta\lambda^N(t) &= \sum_{l=0}^{N} c_l \phi_l(t) \end{aligned} \tag{43}$$

The derivative $\delta\dot{x}^N$ and $\delta\dot{\lambda}^N$ in terms of $\delta x^N(t)$ and $\delta\lambda^N(t)$ at the collocation points t_l using a matrix multiplication are

$$\delta\dot{x}^N(t_k)=\sum_{l=0}^{N}\delta x(t_l)\dot{\phi}_l(t_k)=\sum_{l=0}^{N}D_{kl}\delta x(t_l)=\sum_{l=0}^{N}D_{kl}a_l \tag{44}$$

$$\delta\dot{\lambda}^N(t_k)=\sum_{l=0}^{N}\delta\lambda(t_l)\dot{\phi}_l(t_k)=\sum_{l=0}^{N}D_{kl}\delta\lambda(t_l)=\sum_{l=0}^{N}D_{kl}c_l \tag{45}$$

where D_{kl} are entries of the $(N+1)\times(N+1)$ differentiation matrix D.

The Eq. (29) and Eqs. (33) and (34) are discretized and transformed into the following algebraic equations in terms of the coefficients a, b and c at the LGL nodes, t_k:

$$b_k=-R^{-1}(\tau)B^T(\tau)c_k \tag{46}$$

$$\begin{aligned}\sum_{l=0}^{N}D_{kl}a_l-\frac{\tau_f-\tau_0}{2}(A_ka_k-B_kR^{-1}B^Tc_k)=0\\ \sum_{l=0}^{N}D_{kl}c_l+\frac{\tau_f-\tau_0}{2}(Q_ka_k+A_k^Tc_k)=0\end{aligned} \tag{47}$$

where for a generic matrix $A(t)$, the notation A_k denotes $A(t_k)$, and $k=0, 1, \cdots, N$. Also the 0 is the zero vector of approximate dimension. From Eqs. (46) and (47)

$$u=M\Lambda \tag{48}$$

$$\begin{aligned}EX-\frac{\tau_f-\tau_0}{2}F\Lambda=0\\ \frac{\tau_f-\tau_0}{2}GX+H\Lambda=0\end{aligned} \tag{49}$$

In the above, $0_{k\times n}$, $0_{n\times n}$, and I_n are $k\times n$, $n\times n$ zero matrix, and $n\times n$ unity matrix, respectively. The initial and final conditions are

$$a(0)=\delta x_0=a_0 \tag{50}$$

$$c(N)=P_f\delta x_N=P_fa_N \tag{51}$$

The block matrix form of Eqs. (49) is

$$\begin{bmatrix}\tilde{E} & -\frac{\tau_f-\tau_0}{2}\tilde{F}\\ \frac{\tau_f-\tau_0}{2}\tilde{G} & \tilde{H}\\ \tilde{P}_1 & \tilde{P}_2\end{bmatrix}\begin{bmatrix}X\\ \Lambda\end{bmatrix}\equiv Vz=\begin{bmatrix}0\\0\\0\end{bmatrix} \tag{52}$$

where, $z^T=[X^T, \Lambda^T]$. $n\times n(N+1)$ matrices $\tilde{P}_1$ and $\tilde{P}_2$ are

$$\begin{aligned}\tilde{P}_1=[0_n, \cdots, 0_n, P_f]\\ \tilde{P}_2=[0_n, \cdots, 0_n, -I_n]\end{aligned} \tag{53}$$

When V is present as $V=[V_0\ V_e]$

$$V_0a_0+V_ee=0 \tag{54}$$

where vector e is defined as

$$e=[a_1^T, a_2^T, \cdots, a_N^T, c_0^T, \cdots, c_N^T]^T \tag{55}$$

From Eq. (54), e is derived as

$$e=-V_e\backslash V_0a_0=Wa_0 \tag{56}$$

Since $z=[a_0, e]^T$, z is

$$z=\begin{bmatrix}X\\ \Lambda\end{bmatrix}=\begin{bmatrix}I_n\\ W\end{bmatrix}a_0\equiv\begin{bmatrix}W_1\\ W_2\end{bmatrix}a_0 \tag{57}$$

The set of control variables obtained from Eq. (48) is

$$U=M\Lambda=MW_2a_0 \tag{58}$$

If the initial states are known, the states, costates and controls at the LGL points can be solved from Eqs. (57) and (58), and the values of variables at instants of time between the LGL points can be obtained by interpolation. It should be noticed that we obtained these solutions without any integration or iterations. Regarding the difference between the current states and reference states as the new initial states, Eq. (58) constitutes a close loop control law that can be rapidly performed in the real ime manner.

4.3 Application of PLM into re-entry problem

For each state and control vector, N th degree interpolating polynomials (Elnagar et al., 1995) for RE problem can be approximated as the drag acceleration function with v;

$$D^N(v)=\sum_{l=0}^{N} D(v_l)\,\eta_l(\nu)$$
$$D'^N(v_k)=\sum_{l=0}^{N} D_{kl}^{(1)} D(v_l) \tag{59}$$
$$D''^N(v_k)=\sum_{l=0}^{N} E_{kl}^{(2)} D(v_l)$$

where $E^{(1)}$ and $E^{(2)}$ are first and second order differentiation matrix, respectively.

The range constraint based on the PLM from Eq. (11) is

$$s=\frac{v_0-v_N}{2}\sum_{l=0}^{N}\frac{v_l}{D_l}\,w_l \tag{60}$$

where w_l is weighting.

5. Numerical Results

This chapter shows the reference trajectory by an optimization and the tracking performance onto it. All physical and aero-coefficients data used in this simulation is from Lu (1997).

$$m=104{,}305\ \mathrm{kg},\ S=391.22\ \mathrm{m}^2$$

The aerodynamic coefficients C_L, C_D for the basic vehicle are given in tabulated data as functions of Mach number and angle of attack. For the reference drag trajectory, the coefficients are approximated by fitting the data in hypersonic regimes with

$$C_L=-0.041065+0.016292\alpha+0.00026024\alpha^2 \tag{61}$$
$$C_D=0.080505-0.03026C_L+0.86495C_L^2 \tag{62}$$

The pre-designed angle of attack is 40 deg from $v=7450$ m/s to $v=4570$ m/s for protection of total heating accumulated in the airframe, and then reduced to 14 deg monotonically from $v=4570$ m/s to $v=760$ m/s where the handover to the terminal area energy management system takes place.

The atmospheric entry point is at an altitude of 1222.155 km, the earth relative velocity 7450 m/s and the flight path angle -0.5 deg at this point. The reference drag acceleration is generated by the Matlab-code fmincon which use the SQP algorithm, the elapsed time by Pentium 4 1.6 GHz-CPU is 15.06 sec.

The integration is processed until the final velocity of 760 m/s. At that time, altitude is 22.165 km and the flight path angle is -6.899 deg. Fig. 2 shows the comparison between the reference trajectory which is optimized with all constraints, and the real one from Eqs. (1)-(3). The number of iteration is 104, and reference range is 3000 km. The history of control input σ is shown in Fig. 3.

The time-to-go guidance scheme in Ref. (Elnagar and Razzaghi, 1997) can be explained as followings. First set up of optimization data about states, control variable, then, the selection of initial perturbations δx_0. The actual trajectory is then controlled by $U=\delta U+U^*$ with the nonlinear dynamics governed by system Eqs. (1)-(3), where the asterisk denotes the reference value. The next perturbations δx are generated from $\delta x=x-x^*$, not from Eq. (24), where x is

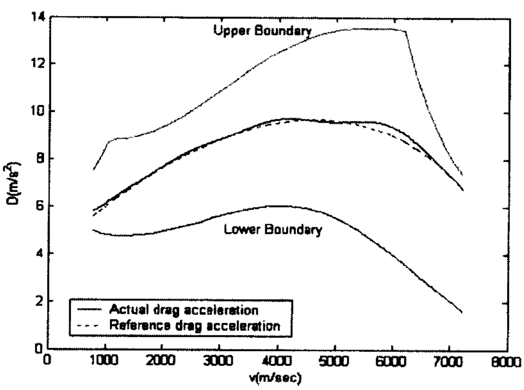

Fig. 2 Time histories of Drag Acceleration

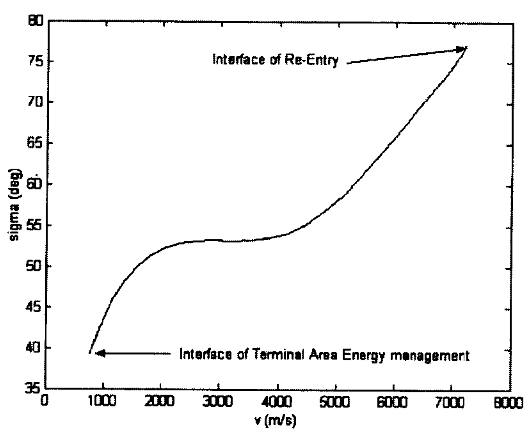

Fig. 3 Time history of Bank angle

the state response from nonlinear dynamics with $U=\delta U+U^*$. This procedure to the final time is repeated. The number of LGL point used in this simulation is 30. Table 1 and 2 represent the difference between the actual and reference states according to three cases which are defined

Table 1 Differences of states for the open-loop guidance

Cases	Δr_0 (km)	ΔV_0 (m/s)	$\Delta\gamma_0$ (deg)	Open loop			
				$\Delta\gamma_f$ (km)	ΔV_f (m/s)	$\Delta\gamma_f$ (deg)	Δs_f (km)
1	0.5	80	0.9	5.168	315.18	2.664	379.59
2	−0.5	−80	−0.9	−4.728	−202.239	−3.981	−296.86
3	1.7	50	0.3	1.656	88.346	1.072	115.21
4	−1.7	−50	−.0.3	−1.614	−76.47	−1.200	−106.2

Table 2 Differences of states for the closed-loop guidance

Cases	Δr_0 (km)	ΔV_0 (m/s)	$\Delta\gamma_0$ (deg)	Closed loop			
				$\Delta\gamma_f$ (km)	ΔV_f (m/s)	$\Delta\gamma_f$ (deg)	Δs_f (km)
1	0.5	80	0.9	−1.394e-3	0.468	0.002	100.83
2	−0.5	−80	−0.9	1.7488e-3	−0.894	−0.004	−83.92
3	1.7	50	0.3	−0.986	0.313	0.001	59.44
4	−1.7	−50	−0.3	0.994	−0.527	−0.002	−56.74

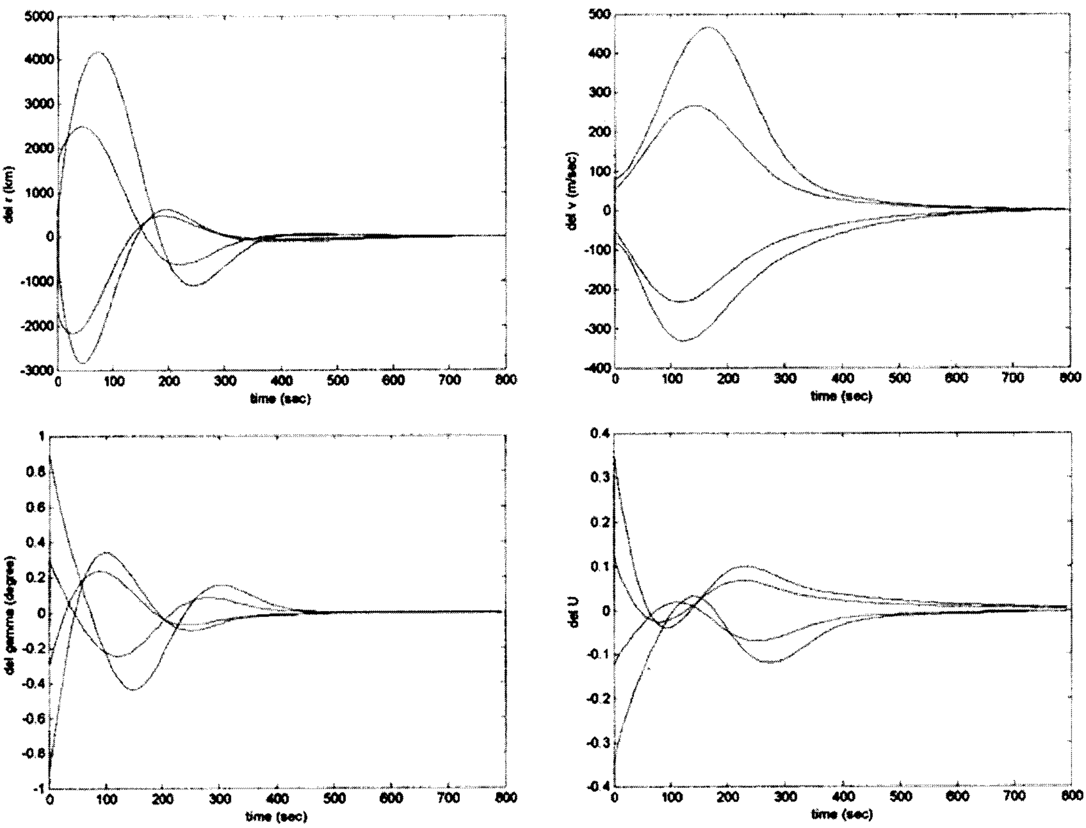

Fig. 4 Time variations of the states and control variable

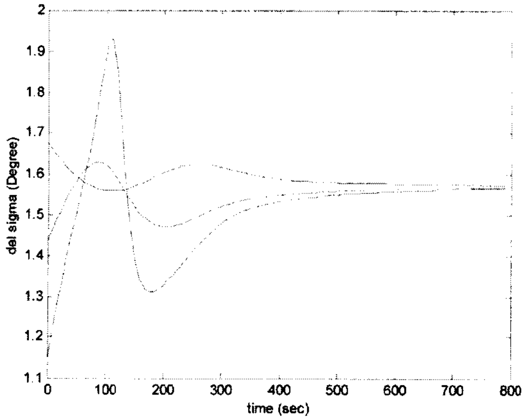

Fig. 5 Time variations of the bank angle

with the initial perturbations. Table 1 is for open loop guidance and Table 2 is for closed loop guidance. we can verify the more accurate results in closed loop system. Fig. 4 represents the convergent performance of states and control variable in linear system. The bank angle variation in linear system is represented in Fig. 5. Successful trajectory regulation should lead to $\Delta x \rightarrow 0$, and thus $\Delta u \rightarrow 0$, provided the trajectory dispersions are not so large as to invalidate the linerization approximation or cause destabilizing control saturation.

6. Conclusions

Among the many guidance schemes, this paper introduce the inverse dynamics method with Legendre polynomial. This is one of collocation-type methods for quadratic optimal control problem, can be called spectral Legendre method. By this method, LTV systems is reduced to the linear TPBVP, then is transformed to a linear algebraic equations. Its solving requires only some matrix operations without any integration or iterations. Since the law has an approximate analytical expression associated with the initial states, it can be rapidly performed in the real time manner.

References

Alberto Cavallo, 1996, "Atmosphere Re-entry Control for Low Lift/Drag Vehicle," *Journal of Guidance, Control, and Dynamics*, Vol. 19, No. 1, pp. 47~53.

Axel J. Roenneke, 1993, "Trajectory Control for a Low-Lift Re-Entry Vehicle," *Journal of Guidance, Control, and Dynamics*, Vol. 16, No. 5, pp. 927~933.

Baker, C. D., Causey, W. E. and Ingram, H. L., 1971, "Mathematical Concepts and Historical Development of the MOSCOT Guidance Technique for Space Vehicle," NASA Technical Memorandum, NASA TM-44408.

Bryson, A. E., 1975, *Applied Optimal Control*, Hemisphere Publishing Corporation.

Canuto, C., Hussaini, M. Y., Quarteroni, A. and Zang, T. A., 1988, *Spectral Methods in Fluid Dyanmics*, Springer, New York.

Elnagar. J., Kazemi, M. A. and Razzaghi, M., 1995, "The Pseudospectral Legendre Method for Discretizing Optimal Control Problem," *IEEE Transcations on Automatic Control*, Vol. 40, No. 10, pp. 1793~1796.

Frank J. Regan and Satya M. Anandakrishnan, 1993, *Dynamics of Atmospheric Re-entry*, AIAA.

Frank P. Incropera and David P. DeWitt, 1985, *Introduction to Heat Transfer*, John Wiley & Sons.

Gamal N. Elnagar and Mohsen Razzaghi, 1997, "A Collocation-Type Method for Linear Quadratic Optimal Control Problem," *Optimal Control Application & Methods*, Vol. 18, pp. 227~235.

Han, B. K., Chung, K. and Han, D. S., 1989, "Vibration Analysis on Plates By Orthogonal Polynomial," *KSME International Journal*, Vol. 3, No. 2, pp. 95~102.

Harpold, J. C. and Graves, C. A., Jr., 1979, "Shuttle Entry Guidance," *Journal of Astronautical Sciences*, Vol. 26, No. 3, pp. 239~268.

Jinhee Lee, 2003, "Application of the Chebyshev-Fourier Pseudospectral Method to the Eigenvalue Analysis of Circular Mindlin Plates with Free Boundary Conditions," *KSME International Journal in Korea*, Vol. 17, No. 10, pp. 1458~1465.

Jinhee Lee, 2003, "In-Plane Free Vibration Analysis of Curved Timoshenko Beams by the

Pseudospectral Method," *KSME International Journal in Korea*, Vol. 17, No. 8, pp. 1156~1163.

Jong-Phil Kim, and Jeha Ryu, 2002, "Inverse Kinematic and Dynamic Analyses of 6-DOF PUS Type Parallel Manipulators," *KSME International Journal in Korea*, Vol. 16, No. 1, pp. 13~23.

Lee, D. W. and Cho, K. R., 2002, "Reference Trajectory Analysis and Trajectory Control by Bank Angle for Re-Entry Vehicle," *KSME International Journal in Korea*, Vol. 16, No. 6, pp. 745~756.

Lu. P., 1997, "Entry Guidance and Trajectory Control for Reusable Launch Vehicle," *Journal of Guidance, Control, and Dynamics*, Vol. 20, No. 1, pp. 143~149.

Regan, F. J., 1993, *Dynamic of Atmospheric Re-entry*, AIAA Education Series.

Sim, W. G. and Kim, J. M., 1996, "Application of Spectral Collocation Method to Conduction and Laminar Forced Heat Convection in Eccentric Annuli," *KSME International Journal*, Vol. 10, No. 1, pp. 04~104.